WOOD RESEARCH doi.org/10.37763/wr.1336-4561/67.5.823836
e-ISSN 2729-8906
67(5): 2022 823-836 pp.

INFLUENCE OF VACUUM IMPREGNATION PRESSURES ON THE NANOMECHANICAL CHARACTERISTICS AND PHOTOCATALYTIC PERFORMANCE OF NANO TIO_2-FURFURYL ALCOHOL/BALSA WOOD-BASED COMPOSITES

GANG ZHU, HUI LI, KUNYONG KANG, XUPENG ZHANG, SHUDUAN DENG
SOUTHWEST FORESTRY UNIVERSITY
P.R. CHINA

(RECEIVED MARCH 2022)

ABSTRACT

In this work, a nano TiO_2-FA/balsa wood-based composites were successfully fabricated by mechanical stirring assisted vacuum impregnation method, and the influence of different impregnation pressures on the microstructure, nanomechanical characteristics and photocatalytic performance of obtained composites were investigated. Results show that the nano TiO_2-FA compound modifier was impregnated in the tracheid and attached to the wood cell walls. SEM revealed that the size of TiO_2 nanoparticles grow larger as the impregnation pressure increases, and the presence of TiO_2 globules with some areas agglomerated on the wood cell wall surface. Compared with the unmodified wood, the elastic modulus of cell walls for nano TiO_2-FA/balsa wood composites prepared under 0.45 MPa significantly increased by 160.5%, and the hardness improved from 0.36 ± 0.04 GPa to 0.84 ± 0.08 GPa. Furthermore, the UV-Vis showed that the composite exhibited a high removal rate of methylene blue (10 $mg \cdot L^{-1}$), up to 88.74% within 240 min.

KEYWORDS: Wood-based composite, nano TiO_2-furfuryl alcohol compound modifier, vacuum impregnation, nanomechanical characteristics, photocatalytic performance.

INTRODUCTION

Balsa wood with low density, sufficient porosity, and good mechanical stability, make it the lightest commercial timber available (Osei-Antwi et al. 2012, Kotlarewski et al. 2016). The low density is extremely valuable in applications that require lightweight materials with good mechanical performance. Therefore, balsa wood is one of the preferred core materials in structural sandwich panels for wind turbine blades, sporting equipment, boats and aircraft (Kwon et al. 2012, Midgley et al. 2010). However, balsa wood also suffers from some less favorable

characteristics such as dimensional instability, susceptibility to fungal attack under humid conditions, photodegradation, and poor thermal stability (Li et al. 2018). Hence, many modification techniques have been proposed to improve the physical, chemical and biological properties of balsa wood (Evans et al. 2008). In recent years, with the development of nanotechnology and other advanced technologies, strategies for designing functional wood-based materials via the simple preparation method have received increasing attention in the field of wood materials (Toivonen et al. 2015, Norgren et al. 2014, Tingaut et al. 2012). Many researchers from all over the world have been using modification and functionalization treatments to improve the natural hierarchical structures and attempt to make them useful in many newly developed fields, such as sewage treatment (Chen et al. 2017a, Fu et al. 2018, Guan et al. 2018, Cheng et al. 2020), solar-powered desalination systems (Zhu et al. 2017, Liu et al. 2017), energy storage (Chen et al. 2017b, Luo et al. 2017) and electronic devices (Chen et al. 2018, Tang et al. 2018, Lang et al. 2018).

Furfuryl alcohol (FA) is a low-molecular organic chemical with strong polarity, derived from the hydrolysate of pentosan-rich agricultural waste (Wang et al. 2006). The stable furan ring structure and hydroxymethyl make furfuryl alcohol have better heat, water resistance and high activity. The previous studies have indicated that FA has a good affinity for wood and easily enters the wood cell wall owing to its swelling effect (Dong et al. 2020). Therefore, furfurylation has been used in wood modification, in which wood is impregnated with furfuryl alcohol (FA) and acidic catalysts. The impregnated wood is then polymerized in-situ at elevated temperature, resulting in so-called “furfurylated wood”, a wood-polymer composite with enhanced mechanical properties, excellent dimensional stability, and good resistance to biological degradation (Li et al. 2015). FA modification as a non-toxic and non-polluting wood modification technology has good application prospects in wood modification. Additionally, the photocatalytic performance of modified wood was remarkably improved by the TiO_2 inorganic nanoparticles modification in a previous study. For example, Luo synthesize TiO_2 wood charcoal composites photocatalysts by using the wood tissue as charcoal resources and bio-template. The results showed that the prepared composites had extraordinary adsorption ability for BPA and good photocatalytic activity (Luo et al. 2015). Ye et al. (2020) reported Nano-TiO_2/insoluble wood flour composite was successfully prepared using insoluble wood flour as bio-carrier and dissolved components as the accelerant. However, there are some drawbacks in these modified strategies, which it is difficult to co-enhancement of mechanical properties and photocatalytic performance. Therefore, it is highly desirable to use efficient methods for developing novel functional wood materials with a synergistic enhancement effect (Hazarika et al. 2014).

In this work, we developed a balsa wood-based functional composite based on furfuryl alcohol treatment and nano TiO_2 modified through mechanical stirring assisted vacuum impregnation method. The morphologies and structures of nano TiO_2-FA/balsa wood composites fabricated under different vacuum impregnation pressures are characterized by using X-ray diffraction (XRD), Fourier transforms infrared spectroscopy (FTIR) and scanning electron microscopy (SEM). In addition, the micromechanical properties and photocatalytic performance of obtained composites were observed by nanoindentation analysis and of degradation methylene blue (MB) test. The results showed that the nano TiO_2-FA compound modifier was successfully

loaded onto the surface of the wood cell walls. Compared with the blank balsa wood scaffold, the nanomechanical characteristics and photocatalytic performance of obtained composites have substantially co-enhancement improved.

MATERIAL AND METHODS

Materials

Native balsa wood (Ochroma pyramidale) was purchased from Xuhong Materials Company (China). In this work, the sapwood and corewood from a balsa wood with uniform anatomical structure 20 mm (L) × 20 mm (T) × 10 mm (R) were selected to minimize the variability in the morphological structure. This avoids the issue of unrepresentative statistical data due to variations in wood properties. For the preparation of nano TiO_2-FA/wood-based composites materials, the materials used were furfuryl alcohol (99%, $C_5H_6O_2$), nanosize danatase titanium dioxide (99.8%, nano TiO_2) with a particle size of 20 nm, maleic anhydride (99%, $C_4H_2O_3$), sodium hexametaphosphate (99%, $(NaPO_3)_6$), sodium tetraborate (99.5%, $Na_2B_4O_7 \cdot 10H_2O$) and KH560 (99%, $C_9H_{20}O_5Si$). For photocatalytic degradation, methylene blue dye (82%, $C_{16}H_{18}ClN_3Cl$) was used. All chemicals used were supplied by the Aladdin Chemical Reagent, China. In this experiment, all the chemical agents were of analytical grade and were used without further purification.

Synthesis of nano TiO_2-FA compound modifier

TiO_2-FA/balsa wood composite was prepared with reference to the method reported in the literature with slight modifications (Dong et al. 2021). The impregnation solution with an FA mass fraction of 30% was prepared according to the mass ratio of furfuryl alcohol: maleic anhydride: borax (1 : 0.05 : 0.01). Subsequently, 0.6 g of sodium hexametaphosphate was weighed and dissolved in 100 mL of deionized water, 2 g of nano titanium dioxide was added, and 2% of KH560 ethanol solution was doped under high-speed stirring, and the above two solutions were mixed and stirred for 10 min to obtain the nano TiO_2-FA composite impregnation solution.

Preparation of the nano TiO_2-FA/balsa wood-based composites

The nano TiO_2-FA/balsa wood-based composites were prepared via mechanical stirring assisted a vacuum impregnation process. First, the dried balsa wood specimens were placed into the vacuum impregnation device and evacuated for 30 min (−0.1 MPa). Afterward, the nano TiO_2-FA composite impregnation solution was transferred into an above device and the balsa wood specimens were immersed in the solution. The device was sealed and then the samples (three corewood, three sapwood for each group) were treated by vacuum impregnation at different vacuum pressures (0.4, 0.45, 0.5, 0.55, and 0.6 MPa) for 2 h. A total of 30 samples were impregnated under the impregnation pressure range of 0.4–0.6 MPa, thereby ensuring the consistency of the preparation conditions and process. To ensure the nano TiO_2-FA composite impregnation solution evenly dispersion, the impregnation process proceeded with constant stirring using a magnetic stirrer. Subsequently, the prepared samples were washed with

deionized water to remove any residual chemicals and put into a constant temperature drying oven at 103°C for 24 h. Thus, the nano TiO_2-FA/balsa wood composites were obtained.

Characterization

Phase identification of nano TiO_2-FA/wood-based composites was analyzed by X-ray diffractometry (XRD, Ultima IV, Rigaku, Japan), with Ni-filtered CuKα radiation, at 40 mA and 40 kV. Fourier-transform infrared spectroscopy (FTIR) spectra (KBr technique) were recorded (IS50, Nicolet, America) with a resolution of (2 cm^{-1}), and the transmittance range of the scan was 4000 cm^{-1} to 400 cm^{-1}. The morphology and microstructure were characterized via field-emission scanning electron microscopy (HITACHI S4800, Tokyo, Japan) with a link EDAX system for local chemical composition analyses. Wood cross-sections were prepared using a microtome (REM-710, Tokyo, Japan).

Nanoindentation tests

The ISO standard method (ISO 14577-4: 2016) for detection of the nanoindentation test (2016). A triboindenter (Bruker Hysitron TI980, Germany) with a Berkovich diamond tip and a radius less than 100 nm was used for indenting. The temperature and relative humidity of the sample chamber was kept at 23 ± 0.5°C and 40 ± 0.5%, respectively. Samples were put into the chamber at least 24 h before indenting, to minimize thermal shifts during testing. Fig. 1 shows the images before and after nanoindentation testing on an area of the wood cell wall of nano TiO_2-FA/balsa wood-based composites. The procedure started with selecting a target region under a light microscope which is integrated into the instrument. The indenter tip was then used to acquire an image of the wood cell wall, from which the locations to be indented were carefully selected. The residual indentations were imaged again with the same tip. A three-segment load ramp was adopted. The target peak load and loading/unloading rates were 500 μN and 50 $\mu N \cdot s^{-1}$ for all of the tests, respectively. After attaining the peak load, the indenter was held at a constant load for 2 s. The elastic modulus (E_s) of elasticity and hardness (H) of the materials were calculated using Eqs. 1 and 2 as follows:

$$H = \frac{F_{max}}{A} = \frac{F_{max}}{24.5 h_c^2} \quad \text{(GPa)} \quad (1)$$

$$E_s = \left(\frac{1-v_s^2}{E_r} + \frac{1-v_i^2}{E_i} \right)^{-1} \quad \text{(GPa)} \quad (2)$$

where: F_{max} is the load measured at a maximum depth of penetration in an indentation cycle (μN); A is the projected contact area (nm^2); and hc is the contact depth of the indentation; v_s (0.422) and v_i (0.07) are the Poisson's ratios of the specimen and indenter, respectively; E_i is the modulus of the diamond indenter (1141 GPa).

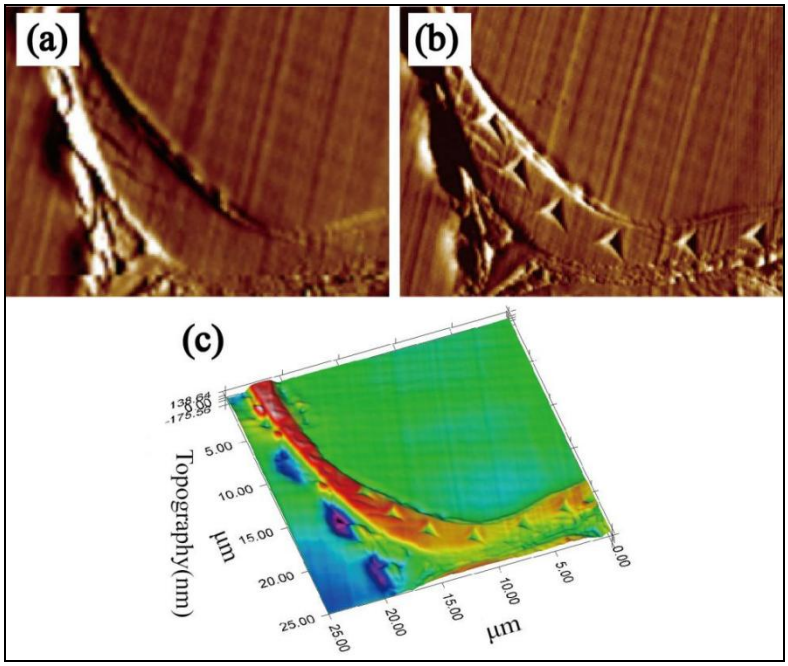

Fig. 1: In situ imaging nanoindentation testing on the nano TiO_2-FA/balsa wood-based composites: (a) scanned image of the cell wall before indentation; (b) scanned image of the cell wall after indentation; (c) 3D image of cell wall after nanoindentation.

Photocatalytic tests

The photocatalytic experiments were conducted as follows. Amount of 0.1 g of photocatalyst and 100 mL methylene blue (MB) solution (10 $mg \cdot L^{-1}$) were put into a quartz beaker. The mixture was stirred in dark conditions for 60 min to reach the adsorption equilibrium and then placed under a UV light away from the beaker about 10 cm. The suspension was stirred vigorously for 60 min under dark conditions, and the UV lamp away from the beaker about 10 cm was turned on for the catalytic reaction after reaching the adsorption-desorption equilibrium. At given intervals, the suspension was withdrawn and centrifuged to remove the dispersed sample powder. The concentration of the clean transparent solution was determined by measuring the absorbance of MB at 665 nm (UH-5300, HITACHI, Japan). The changes in maximum absorption vs. irradiation time (C/C_0 vs. t) reflect the MB concentration decrement.

RESULTS AND DISCUSSION

Characterization of nano TiO_2-FA/balsa wood-based composites

To study the phase composition, XRD analysis was carried out for the five nano TiO_2-FA/balsa wood composites impregnated with the vacuum impregnation treatment under different pressure, the results are shown in Fig. 2. The analytical results show that the unmodified balsa wood sample exhibited two obvious diffraction peaks respectively at 16.1° and 22.1°, which was consistent with the characteristic diffraction peak of cellulose. However, it is worth noting that the diffraction peak of nano TiO_2-FA/balsa wood composites was well consistent with the characteristic diffraction peaks of anatase TiO_2 (25.4°, 37.8°, and 48.0°) and cellulose (22.1°), which indicated that the sample of composites was composed of anatase TiO_2 and wood

flour, and the TiO_2 structure is not destroyed during the vacuum impregnation treatment(Ye et al. 2020).

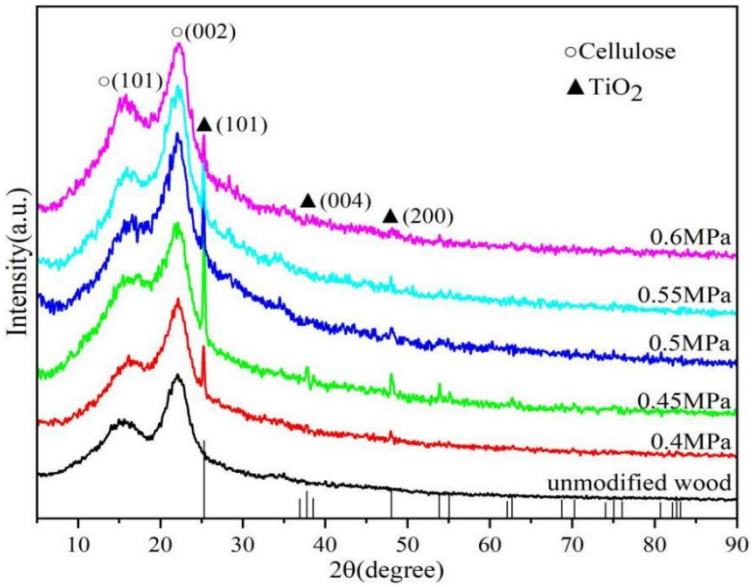

Fig. 2: XRD patterns of unmodified wood and nano TiO_2-FA/balsa wood-based composites by vacuum impregnation treatment under different pressures.

Furthermore, with the rise of vacuum pressure, the diffraction peaks of 16.1° exhibited a trend of decreasing first and then increasing. Specifically, the (101) crystal plane peak intensity of the cellulose is obviously decreased when the vacuum pressure increased from 0.4 MPa to 0.5 MPa. This is ascribed to the fact that lots of FA entering into the wood cells partially up-taken into the cellulose amorphous regions and reacted with the hydroxyl groups in the amorphous regions, which causes a distinct decrease in cellulose as a percentage of the balsa wood and leads to a reduction in diffraction intensity (Hazarika et al. 2014). On the contrary, it should be noted that the diffraction peaks develop an opposite trend with a further increase in pressure. It is owing to the clear agglomerations of TiO_2 nanoparticles and the average grain size growth significantly took place (Fig. 4g), which suppressed the content of cellulose decrease and thus led to an increase in peak intensity corresponding to (101) crystal plane.

The chemical composition of the unmodified wood and nano TiO_2-FA/balsa wood composites prepared at different vacuum pressures were measured by the Fourier transform infrared, which is shown in Fig. 3. It can be seen that the absorption peak at 3420 cm^{-1} is the OH stretching vibration and the peak at 2929 cm^{-1} is the band for C-H vibration from CH and CH_2 in cellulose and hemicellulose (Fig. 3a). A bending vibrational peak of C–H bonds in cellulose and hemicellulose molecules was observed at 1370 cm^{-1}. Additionally, the spectra of samples after FA treatment showed some notable changes due to the incorporation of FA. In detail, the bands at 1714 cm^{-1} were related to the ring opening of poly furfuryl alcohol, and a small band at 1561 cm^{-1} also corresponded to the skeletal vibration of 2,5-disubstituted furan rings. More importantly, the degradation of the cellulose and hemicellulose by the acidic modification solution, which resulted that the peak at 1058 cm^{-1} representing the C-O bond in hemicellulose

or cellulose, and the peaks at 1735 cm^{-1} representing the conjugated C=O stretching bands are weakened. In brief, all of these pointed out that the FA treatment had some effect on the structure of balsa wood. Furthermore, in contrast to balsa wood, the higher strength band of Ti-O was seen at 585 cm^{-1}, indicating the attachment of TiO_2 on the balsa wood cellular lumen (Fig. 3b). The new peaks resulting from FTIR analysis show that the nano TiO_2-FA/balsa wood composites have been successfully synthesized, which is also proven by the SEM-EDS analysis.

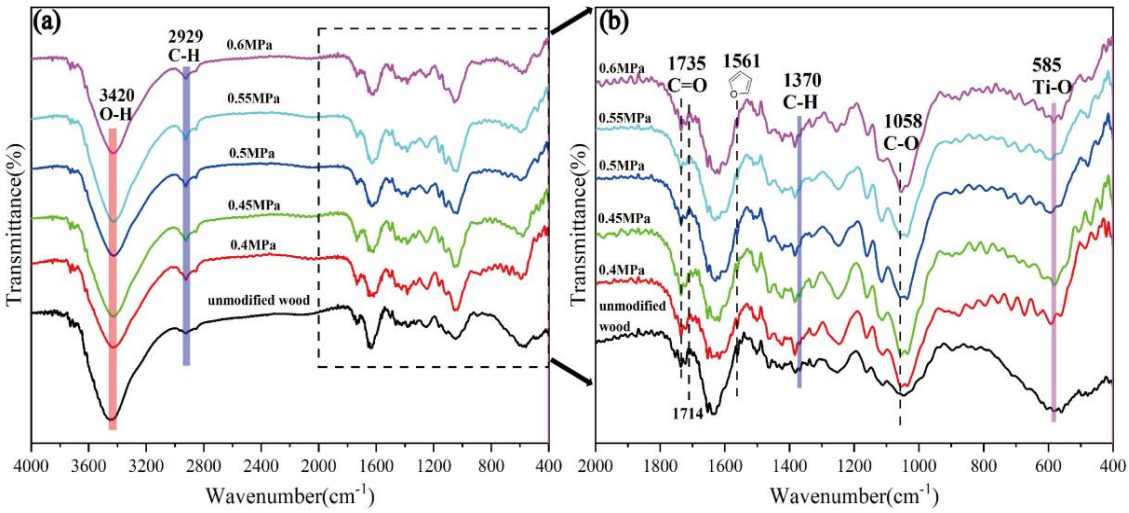

Fig. 3: FTIR spectra of unmodified wood and nano TiO_2-FA/balsa wood-based composites by vacuum impregnation treatment under different pressures: (a) Region from 4000 cm^{-1} to 400 cm^{-1}; (b) region from 2000 cm^{-1} to 400 cm^{-1}.

Fig. 4 shows the microstructures of the unmodified wood and nano TiO_2-FA/balsa wood composites prepared at different vacuum pressures, respectively. The unmodified balsa wood sample exhibited the typical porous anatomical structure of wood, with irregular rounded shapes cell lumina, and close linkage between the wood cells was also observed (Fig. 4a). Additionally, the micromorphology of the balsa wood showed a much more porous structure in wood cell walls compared to other types of wood (Chen et al. 2021, Wang et al. 2021), which was beneficial for the impregnation of the nano TiO_2-FA compound modifier and the interplay between it and the cellulose. After vacuum impregnation treatment, the porous structure was well preserved but exhibited a change in cell lumina. As shown in Fig. 4b, it can be seen that abundant spherical nanoparticles are present on the wood cell wall, and the attachment made the wood cell wall uneven. By EDX energy spectrum analysis (Fig. 4h), we found that the elements C, O and Ti were detected by SEM-EDS. In addition to the C and O elements derived from the wood chemical compositions, the energy dispersive spectrometer (EDS) spectrum also confirmed the existence of Ti elements. This provides a further demonstration that TiO_2 nanoparticles were impregnated in the tracheid and successfully immobilized on the wood substrate.

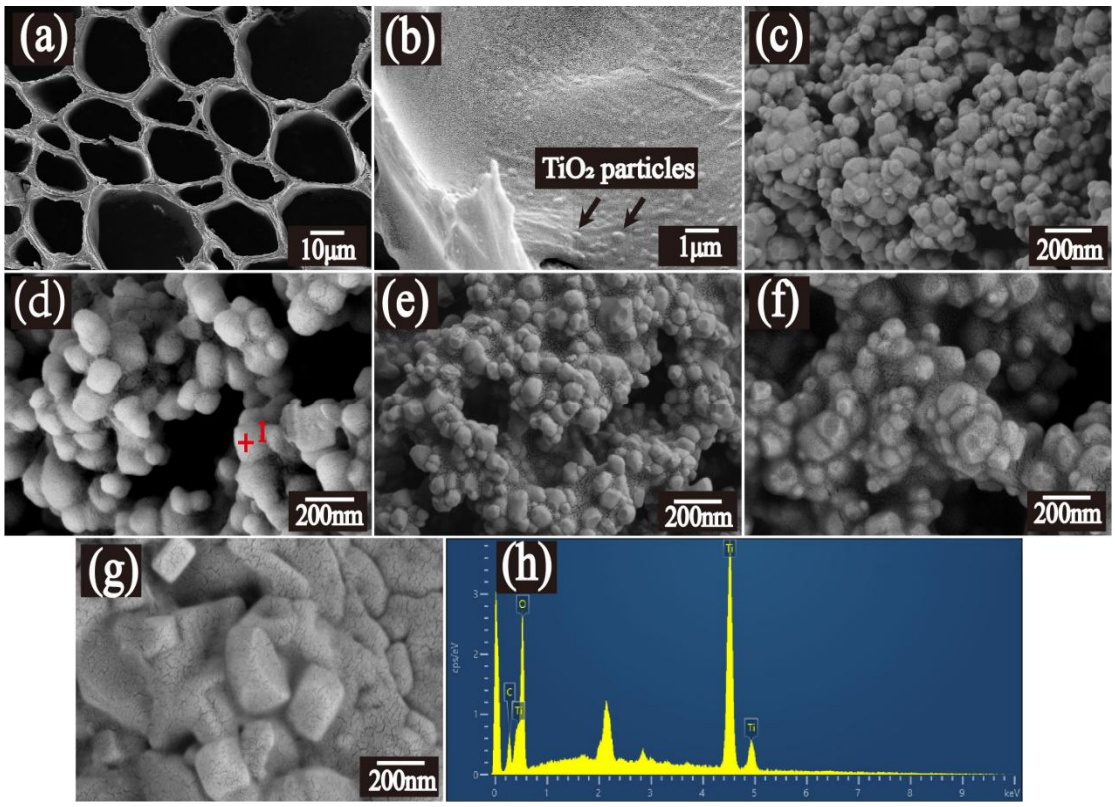

Fig. 4: Transverse section SEM micrographs of unmodified balsa wood (a), high magnification radial section of nano TiO_2-FA/balsa wood composites (b), and radial section images of the composites by vacuum impregnation treatment under different pressures of: (c) 0.4 MPa, (d) 0.45 MPa, (e) 0.5 MPa, (f) 0.55 MPa, (g) 0.6 MPa; (h) EDS spectra and compositions corresponding to Point 1 in Fig. 4d.

A close examination of the sample radial section micrographs revealed several interesting points regarding the structure under an enlarged view. Fig. 4c-g indicates that the impregnation pressure has similar effects on particle size variation and distribution at different vacuum pressures. When the impregnation pressure is 0.4 MPa and 0.45 MPa, the samples exhibited very nearly identical TiO_2 morphology, comparable high coverage with particles of fairly similar size (~130 nm). TiO_2 nanoparticles entered the interior of the wood and attached to the cell wall, many small spherical TiO_2 particle appears to be uniformly dispersed on the wood matrix. A closer look at Fig. 4c-f revealed that the particles size grows larger as the impregnation pressure increases, and the presence of TiO_2 globules with some areas agglomerated on the wood cell wall surface. In contrast, as shown in Fig. 4e (pressure 0.5 MPa), much smaller agglomerates (184 nm and smaller) with spherical shapes are common and appear to be uniformly dispersed within the specimen. However, when the impregnation pressure increased further to 0.6 MPa (Fig. 4g), some nano TiO_2 spherical particles gradually agglomerate into bulk irregular shapes grains (300-400 nm). SEM observations confirmed that the dissolved hemicellulose and low molecular weight cellulose indeed promoted the formation of nano TiO_2.

Nanomechanical characteristics and photocatalytic performance of nano TiO_2-FA/balsa wood-based composites

The nanoindentation technique is a method to determine the mechanical properties of wood cell walls at the nanoscale (Ammann et al. 2014, Wu et al. 2010, Xing et al. 2016, Tze et al. 2007). By the use of nanoindentation techniques, the elastic modulus and hardness of the unmodified wood, furfurylation balsa wood and nano TiO_2-FA/balsa wood composites are shown in Fig. 5. Previous studies have suggested that penetration and polymerization of furfuryl alcohol in wood cavities and even cell wall could improve most properties of modified woods (Li et al. 2015). Fig. 5 shows that relative to untreated wood, the indentation modulus of cell walls for furfurylation balsa wood significantly increased by 125.9% from 8.18 ± 0.77 GPa to 19.90 ± 1.69 GPa and the hardness improved by 108.3% from 0.36 ± 0.04 GPa to 0.75 ± 0.11 GPa. An improvement in the indentation modulus and hardness of furfurylation balsa wood cells demonstrated indirectly but strongly that furfuryl alcohol (FA) can easily penetrate wood cells walls and polymerize in-situ during the vacuum impregnation process, which results in significantly improved physical-mechanical properties.

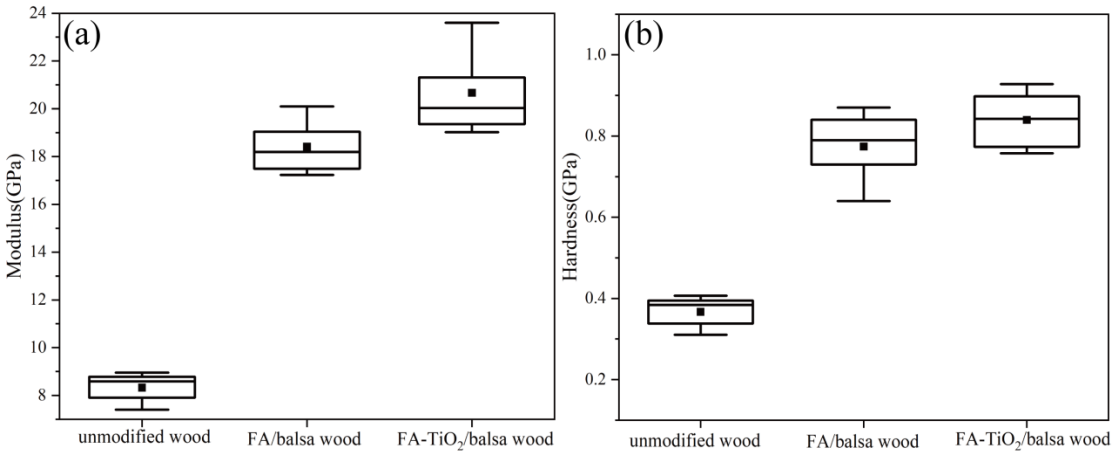

Fig. 5: Elastic modulus (a) and hardness (b) of unmodified wood, FA/balsa wood and nano TiO_2-FA/balsa wood-based composites by vacuum impregnation treatment under 0.45 MPa.

Comparison with furfurylation balsa wood, both the indentation modulus and hardness of nano TiO_2-FA/balsa wood composites fabricated under 0.45 MPa slight additional increases to 21.31 ± 2.29 GPa and 0.84 ± 0.08 GPa, respectively. It is clear that the degree of modification in balsa wood properties mainly depends on the polymer content inside wood cell walls. At the same time, lots of TiO_2 nanoparticles entering into the wood cells partially up-taken into the cellulose amorphous regions and reacted with the hydroxyl groups in the amorphous regions, which results in further improved physical-mechanical properties of balsa wood. Collectively, a positive effect of the multi-incorporation of furfuryl alcohol and TiO_2 nanoparticles into the cell wall of balsa wood on mechanical properties was strongly demonstrated by means of nanoindentation.

The photocatalytic properties of the nano TiO_2-FA/balsa wood composites with different vacuum impregnation pressures for methylene blue (MB) degradation are shown in Fig. 6.

The results show that the adsorption equilibrium is reached within 60 min, and the composite fabricated under 0.45 MPa exhibits an excellent adsorption capacity. Compared with the control, the elimination effectiveness for all the nano TiO_2-FA/balsa wood composites at $\lambda = 665$ nm exhibited a non-ignorable degradation performance of MB. Moreover, from Fig. 6 it is denoted that photocatalytic activity first increases and then decreases with increasing vacuum impregnation pressure. This indicates that there is an optimal vacuum impregnation pressure of the nano TiO_2-FA/balsa wood composites. The degradation rate of MB by the obtained composite under 0.4 MPa is only 66.16% within 240 min, by contrast, the nano TiO_2-FA/composites prepared under 0.45 MPa presents a remarkable degradation performance which achieves much higher to 88.74% with the same time. Notably, when pressure is increased further, photocatalytic activity exhibits a declining trend. When the pressure increases further to 0.6 MPa, the degradation rate of MB distinctly decreased to 80.56% within 240 min. This behavior is mainly attributed to the presence of TiO_2 globules with some areas agglomerated on the wood cell wall surface and transformed to bulk irregular shapes grains (Fig. 4g), which would reduce the specific surface area and cause the decreased number of exposed reactive sites, thereby reducing the photocatalytic activity of the composite.

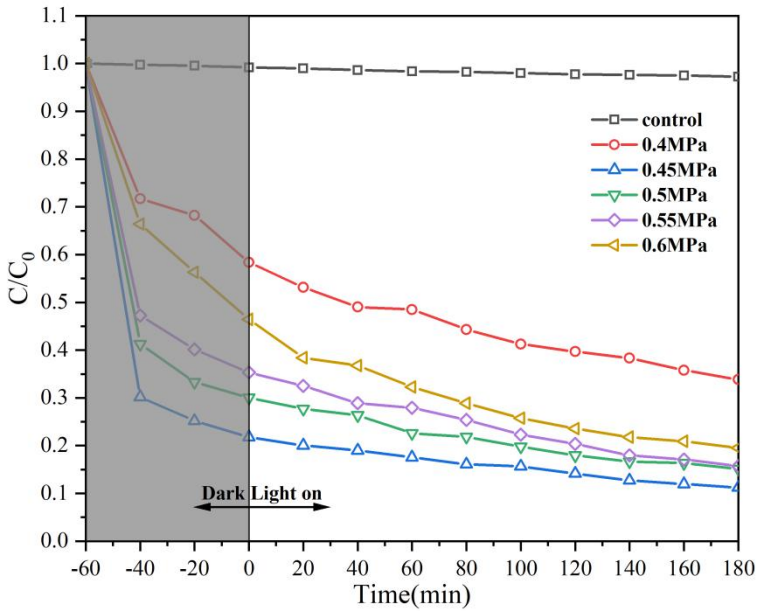

Fig. 6: Photocatalytic activities of the nano TiO_2-FA/balsa wood-based composites by vacuum impregnation treatment under different pressures in the degradation of MB under UV-light irradiation.

CONCLUSIONS

In the present study, the influence of different vacuum impregnation pressures on the microstructure, nanomechanical characteristics and photocatalytic performance of obtained nano TiO_2-FA/balsa wood-based composites were investigated. The conclusions of this study can be summarized as follows: *(1)* The nano TiO_2-FA compound modifier was impregnated in the balsa wood cell wall and successfully immobilized on the wood substrate. Moreover,

the average grain size of TiO_2 nanoparticles grows larger as the impregnation pressure increases, and the presence of TiO_2 globules with some areas agglomerated on the wood cell wall surface, some nano TiO_2 spherical particles gradually agglomerate into bulk irregular shapes grains. *(2)* Compared with unmodified wood, nano TiO_2-FA/balsa wood composites showed optimum comprehensive properties by vacuum impregnation treatment under 0.45 MPa. The elastic modulus of cell walls for nano TiO_2-FA/balsa wood composites fabricated under 0.45 MPa significantly increased from 8.18 ± 0.77 GPa to 21.31 ± 2.29 GPa, and the hardness improved from 0.36 ± 0.04 GPa to 0.84 ± 0.08 GPa. Furthermore, the photocatalytic activity of obtained composite first increases and then decreases with increasing vacuum impregnation pressure. when the impregnation pressure reaches 0.45 MPa, the photocatalytic degradation performance of nano TiO_2-FA/balsa wood composites is up to 88.74% within 240 min, which is obviously higher than that of the degradation rate under the other pressure conditions. The current study offers a stable and sustainable strategy for the fabrication of multifunctional balsa wood-based composites with potential applications in environmental and green building-related fields.

ACKNOWLEDGMENTS

This work was supported by a grant-in-aid from the National Natural Science Foundation of China (No. 31860188), and the Startup Fund for Scientific Research, Southwest Forestry University (No.18210122).The authors also thank the Analytical and Testing Center at Southwest Forestry University for providing experimental facilities.

REFERENCES

1. Ammann, S., Obersriebnig, M., Konnerth, J., Gindl-Altmutter, W., Niemz, P., 2014: Comparative adhesion analysis at glue joints in European beech and Norway spruce wood by means of nanoindentation. International Journal of Adhesion and Adhesives 50: 45-49.
2. Chen, F., Gong, A.S., Zhu, M., Chen, G., Lacey, S.D., Jiang, F., Li, Y., Wang, Y., Dai, J., Yao, Y., 2017: Mesoporous, three-dimensional wood membrane decorated with nanoparticles for highly efficient water treatment. ACS Nano 11(4): 4275-4282.
3. Cheng, Z., Guan, H., Meng, J., Wang, X., 2020: Dual-functional porous wood filter for simultaneous oil/water separation and organic pollutant removal. ACS omega 5(23): 14096-14103.
4. Chen, C., Zhang, Y., Li, Y., Kuang, Y., Song, J., Luo, W., Wang, Y., Yao, Y., Pastel, G., Xie, J., 2017: Highly conductive, lightweight, low-tortuosity carbon frameworks as ultrathick 3D current collectors. Advanced Energy Materials 7(17): 1700595.
5. Chen, C., Song, J., Zhu, S., Li, Y., Kuang, Y., Wan, J., Kirsch, D., Xu, L., Wang, Y., Gao, T., 2018: Scalable and sustainable approach toward highly compressible, anisotropic, lamellar carbon sponge. Chem 4(3): 544-554.

6. Chen, G., He, S., Shi, G., Ma, Y., Ruan, C., Jin, X., Chen, Q., Liu, X., Dai, H., Chen, X., 2021: In-situ immobilization of ZIF-67 on wood aerogel for effective removal of tetracycline from water. Chemical Engineering Journal 423: 130184.
7. Dong, Y., Ma, E., Li, J., Zhang, S., Hughes, M., 2020: Thermal properties enhancement of poplar wood by substituting poly(furfuryl alcohol) for the matrix. Polymer Composites 41(3): 1066-1073.
8. Dong, C., Zhang, S., Wang, J., Chui, Y.H., 2021: Static bending creep properties of furfurylated poplar wood. Construction and Building Materials 269(5): 121308.
9. Evans, P., Matsunaga, H., Kiguchi, M., 2008: Large-scale application of nanotechnology for wood protection. Nature Nanotechnology 3: 577.
10. Fu, Q., Ansari, F., Zhou, Q., Berglund, L.A., 2018: Wood nanotechnology for strong, mesoporous, and hydrophobic biocomposites for selective separation of oil/water mixtures. ACS Nano 12(3): 2222-2230.
11. Guan, H., Cheng, Z., Wang, X., 2018: Highly compressible wood sponges with a spring-like lamellar structure as effective and reusable oil absorbents. ACS Nano 12(10): 10365-10373.
12. Hazarika, A., Maji, T.K., 2014: Properties of softwood polymer composites impregnated with nanoparticles and melamine formaldehyde furfuryl alcohol copolymer. Polymer Engineering & Science 54(5): 1019-1029.
13. ISO 14577-4, 2016: Metallic materials. Instrumented indentation test for hardness and materials parameters. Part 4: Test method for metallic and non-metallic coatings.
14. Kotlarewski, N. J., Belleville, B., Gusamo, B. K., Ozarska, B., 2016: Mechanical properties of Papua New Guinea balsa wood. European Journal of Wood and Wood Products 74(1): 83-89.
15. Kwon, Y., Violette, M., McCrillis, R., Didoszak, J., 2012: Transient dynamic response and failure of sandwich composite structures under impact loading with fluid structure interaction. Applied Composite Materials 19(6): 921-940.
16. Li, J., Zhang, A., Zhang, S., Gao, Q., Chen, H., Zhang, W., Li, J., 2018: High-performance imitation precious wood from low-cost poplar wood via high-rate permeability of phenolic resins. Polymer Composites 39(7): 2431-2440.
17. Liu, K.K., Jiang, Q., Tadepalli, S., Raliya, R., Biswas, P., Naik, R.R., Singamaneni, S., 2017: Wood-graphene oxide composite for highly efficient solar steam generation and desalination. ACS Applied Materials & Interfaces 9(8): 7675-7681.
18. Luo, W., Zhang, Y., Xu, S., Dai, J., Hitz, E., Li, Y., Yang, C., Chen, C., Liu, B., Hu, L., 2017: Encapsulation of metallic Na in an electrically conductive host with porous channels as a highly stable Na metal anode. Nano Letters 17(6): 3792-3797.
19. Lang, A. W., Li, Y., De Keersmaecker, M., Shen, D. E., Österholm, A. M., Berglund, L., Reynolds, J. R., 2018: Transparent wood smart windows: Polymer electrochromic devices based on poly (3,4-ethylenedioxythiophene): poly (styrene sulfonate) electrodes. ChemSusChem 11(5): 854-863.
20. Li, W., Wang, H., Ren, D., Yu, Y., Yu, Y., 2015: Wood modification with furfuryl alcohol catalysed by a new composite acidic catalyst. Wood Science and Technology 49(4): 845-856.

21. Luo, L., Yang, Y., Xiao, M., Bian, L., Yuan, B., Liu, Y., Jiang, F., Pan, X., 2015: A novel biotemplated synthesis of TiO_2/wood charcoal composites for synergistic removal of bisphenol A by adsorption and photocatalytic degradation. Chemical Engineering Journal 262: 1275-1283.
22. Midgley, S., Blyth, M., Howcroft, N., Midgley, D., Brown, A., 2010: Balsa: biology, production and economics in Papua New Guinea. ACIAR Technical Reports Series (73): 98.
23. Norgren, M., Edlund, H., 2014: Lignin: Recent advances and emerging applications. Current Opinion in Colloid Interface Science 19(5): 409-416.
24. Osei-Antwi, M., de Castro, J., Vassilopoulos, A., Keller, T., 2012: Shear mechanical characterization of balsa wood as core material of composite sandwich bridge deck. Construction and Building Materials 41: 231-238.
25. Toivonen, M.S., Kurki-Suonio, S., Schacher, F.H., Hietala, S., Rojas, O.J., Ikkala, O., 2015: Water-resistant, transparent hybrid nanopaper by physical cross-linking with chitosan. Biomacromolecules 16(3): 1062-1071.
26. Tingaut, P., Zimmermann T., Sebe, G., 2012: Cellulose nanocrystals and microfibrillated cellulose as building blocks for the design of hierarchical functional materials. Journal of Material Chemistry 22: 20105-20111.
27. Tang, Q., Fang, L., Wang, Y., Zou, M., Guo, W., 2018: Anisotropic flexible transparent films from remaining wood microstructures for screen protection and Ag NW conductive substrate. Nanoscale 10(9): 4344-4353.
28. Tze, W. T. Y., Wang, S., Rials, T. G., Pharr, G. M., Kelley, S. S., 2007: Nanoindentation of wood cell walls: Continuous stiffness and hardness measurements. Composites Part A: Applied Science and Manufacturing 38(3): 945-953.
29. Wang, H., Yao, J., 2006: Use of poly (furfuryl alcohol) in the fabrication of nanostructured carbons and nanocomposites. Industrial & Engineering Chemistry Research 45(19): 6393-6404.
30. Wang, Z., He, Y., Zhu, L., Zhang, L., Liu, B., Zhang, Y., Duan, T., 2021: Natural porous wood decorated with ZIF-8 for high efficient iodine capture. Materials Chemistry and Physics 258: 123964.
31. Wu, Y., Wang, S., Zhou, D., Xing, C., Zhang, Y., Cai, Z., 2010: Evaluation of elastic modulus and hardness of crop stalks cell walls by nano-indentation. Bioresource Technology 101(8): 2867-2871.
32. Xing, D., Li, J., Wang, X., Wang, S., 2016: In situ measurement of heat-treated wood cell wall at elevated temperature by nanoindentation. Industrial Crops and Products 87: 142-149.
33. Ye, J., Chao, C., Hong, J., 2020: Preparation of a novel nano-TiO_2 photocatalytic composite using insoluble wood flour as bio-carrier and dissolved components as accelerant. Journal of Materials Research and Technology 9(5): 11255-11262.
34. Zhu, M., Li, Y., Chen, G., Jiang, F., Yang, Z., Luo, X., Wang, Y., Lacey, S. D., Dai, J., Wang, C., 2017: Tree-inspired design for high-efficiency water extraction. Advanced Materials 29(44): 1704107.

GANG ZHU*, HUI LI, KUNYONG KANG, XUPENG ZHANG, SHUDUAN DENG*
SOUTHWEST FORESTRY UNIVERSITY
COLLEGE OF MATERIAL SCIENCE AND ENGINEERING
KUNMING 650224
P. R. CHINA
*Corresponding authors: zhugangipm209@163.com and dengshuduan@163.com